Available online at www.sciencedirect.com
SCIENCE DIRECT®
ELSEVIER
Journal of Magnetism and Magnetic Materials 293 (2005) 540–545
Journal of magnetism and magnetic materials
www.elsevier.com/locate/jmmm

Improved paramagnetic chelate for molecular imaging with MRI

Patrick Winter[a], Phillip Athey[b], Garry Kiefer[b], Gyongyi Gulyas[b], Keith Frank[b], Ralph Fuhrhop[a], David Robertson[c], Samuel Wickline[a], Gregory Lanza[a,*]

[a]*Cardiovascular Magnetic Resonance Laboratory, Washington University, 660 S. Euclid Avenue – Campus Box 8086, St. Louis, MO 63146, USA*
[b]*Dow Chemical Co., Freeport, TX, USA*
[c]*University of Missouri Research Reactor, Columbia, MO, USA*

Available online 2 March 2005

Abstract

The relaxivity and transmetallation of two lipophilic paramagnetic chelates incorporated onto perfluorocarbon nanoparticles, i.e., gadolinium-methoxy-tetraazacyclododecane-tetraacetic acid phosphatidylethanolamine (Gd-MeO-DOTA-PE) and gadolinium-methoxy-tetraazacyclododecane-tetraacetic acid triglycine phosphatidylethanolamine (Gd-MeO-DOTA-triglycine-PE (Gd-MeO-DOTA-triglycine-PE)), were compared to a prototypic gadolinium-diethylene-triamine-pentaacetic acid bis-oleate (Gd-DTPA-BOA) paramagnetic formulation. Nanoparticles with MeO-DOTA-based chelates demonstrated higher relaxivity (40% higher for Gd-MeO-DOTA-PE and 55% higher for Gd-MeO-DOTA-triglycine-PE) and less transmetallation than the original Gd-DTPA-BOA-based agent.

Keywords: Magnetic resonance imaging (MRI); Contrast agent; Nanoparticles; Relaxivity; Transmetallation; Chelator; DOTA; DTPA; Perfluorocarbon; Gadolinium

1. Introduction

Molecular imaging is emerging as a sensitive and specific method for the detection and localization of the biochemical signatures of disease. Magnetic resonance imaging (MRI) offers several advantages over other clinical modalities for molecular imaging, including high resolution, non-invasiveness, high anatomical contrast and lack of ionizing radiation. The partial volume dilution effect, which is inherent in MRI, has often led to the failure of targeted contrast agents in vivo [1]. Initial attempts of targeted imaging with MRI focused on coupling gadolinium atoms directly to antibodies or proteins [2,3], but these approaches delivered insufficient paramagnetic material to

*Corresponding author. Tel.: +314 454 8813; fax: +314 454 5265.
E-mail address: greg@cvu.wustl.edu (G. Lanza).

0304-8853/$ - see front matter © 2005 Published by Elsevier B.V.
doi:10.1016/j.jmmm.2005.01.062

effectively decrease local relaxation times, and provided inadequate MR signal enhancement on T_1-weighted images at typical clinical field strengths. Later, ligand-directed macromolecular constructs, such as liposomes [4], nanoparticles [5–7], dendrimers [8], polymers [9], were used to increase gadolinium ion payload at each binding site, which generated in some instances acceptable levels of targeted MRI contrast. The two principal factors for the development of successful targeted paramagnetic contrast agents are the number of gadolinium ions delivered to each binding site, i.e. the paramagnetic payload, and the relaxivity influence provided by each gadolinium [5].

We have previously reported and characterized a paramagnetic lipid-encapsulated perfluorocarbon nanoparticle contrast agent for the sensitive and specific detection and localization of fibrin [5,10] and molecular signatures of angiogenesis [6,7]. These prototype nanoparticles (250 nominal diameter) incorporate a lipophilic chelate, i.e., gadolinium-diethylene-triamine-pentaacetic acid bis-oleate (Gd-DTPA-BOA, metal oriented outward) into the surfactant layer. These relatively large paramagnetic constructs have high relaxivity per gadolinium atom (ion-based relaxivity) due to the slower tumbling rate of the particle in comparison with free gadolinium-diethylene-triamine-pentaacetic acid (Gd-DTPA) [11] and support high surface payloads of metal, typically in excess of 50,000 gadolinium ions per 250 nm particle, providing extremely high relaxivity per particle (particle-based relaxivity). Since biochemical epitopes of interest are often present in nano- or picomolar concentrations, particulate relaxivities around 1,000,000 $s^{-1} mM^{-1}$ are required to achieve acceptable contrast-to-noise at typical clinical field strength (1.5 T) [12].

While Gd-DTPA-BOA nanoparticles have been used effectively to image thrombi [5] and angiogenesis [6,7] in vivo, increases in particulate relaxivity will improve detection of nascent disease even at lower scanning resolution and will reduce the incidence of false-negative studies. In clinical practice, low-resolution detection will be required to interrogate wide regions of interest. Once detected in lower resolution scans, high-resolution molecular imaging can be pursued for diagnosis and quantification.

Unlike the blood-pool paramagnetic chelates, site-specific MR contrast agents circulate longer and accumulate at the target site over time, where they provide persistent signal for several hours. The requisite extended biological half-life of these agents necessitates stable gadolinium chelate complexes to minimize toxicity potential through transmetallation [13,14].

In the present report, we compare the relaxivity and transmetallation potential of gadolinium-methoxy-tetraazacyclododecane-tetraacetic acid (Gd-MeO-DOTA)-based nanoparticles with our previously reported Gd-DTPA-BOA prototype agent.

2. Materials and methods

2.1. Nanoparticle formulation

Nanoparticle contrast agents were produced with methods developed in our laboratory [5,10]. Emulsions comprised 20% (v/v) of perfluorooctylbromide (PFOB; Minnesota Manufacturing and Mining), 2% (w/v) safflower oil, 2% (w/v) of a surfactant commixture, 1.7% (w/v) glycerin and water representing the balance. The surfactant commixture included 58 mol% lecithin (Avanti Polar Lipids), 10 mol% cholesterol (Sigma Chemical Co.), 2 mol% biotinylated dipalmitoyl-phosphatidylethanolamine (Avanti Polar Lipids) and 30 mol% of a paramagnetic lipophilic chelate. One of three different paramagnetic chelates was incorporated onto the nanoparticle surface: gadolinium-diethylene-triamine-pentaacetic acid bis-oleate (Gd-DTPA-BOA; Gateway Chemical Technologies, Fig. 1), gadolinium-methoxy-tetraazacyclododecane-tetraacetic acid phosphatidylethanolamine (Gd-MeO-DOTA-PE; Dow Chemical Co., Fig. 1) or gadolinium-methoxy-tetraazacyclododecane-tetraacetic acid triglycine phosphatidylethanolamine (Gd-MeO-DOTA-triglycine-PE; Dow Chemical Co., Fig. 1).

Particle sizes were determined at 37 °C with a laser light-scattering submicrometer particle sizer (Malvern Instruments). The particle concentrations were calculated from the nominal particle size (i.e., particle volume of a sphere) and the amount of PFOB formulated into the preparation

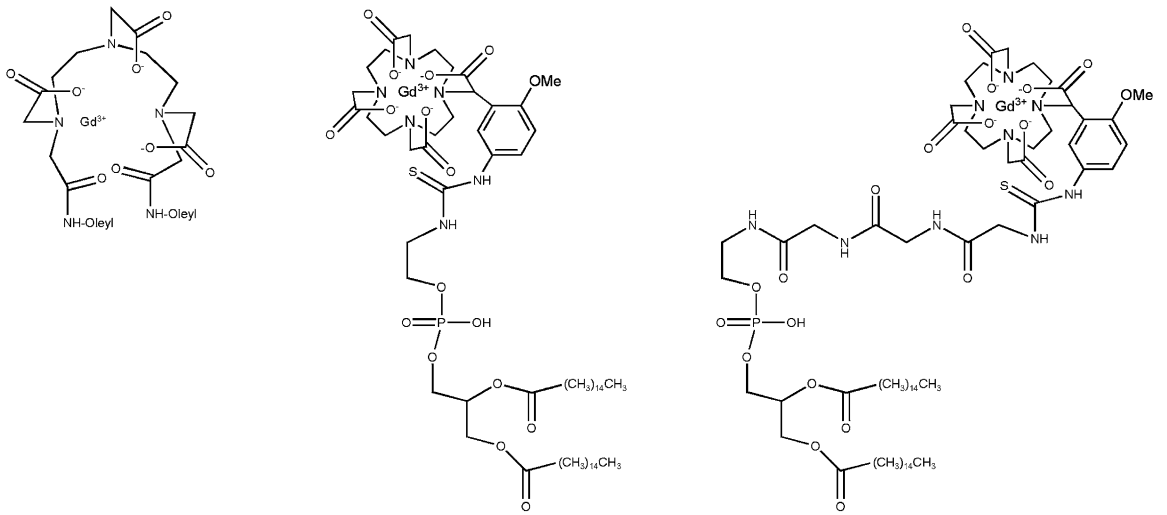

Fig. 1. Chemical structures of Gd-DTPA-BOA (left), Gd-MeO-DOTA-PE (middle) and Gd-MeO-DOTA-triglycine-PE (right).

[12]. The Gd^{3+} content of each nanoparticle formulation was measured with neutron activation analysis [11]. Briefly, lyophilized samples were irradiated with neutrons in a 10 MW nuclear reactor to produce gadolinium-specific radionuclides, which were quantitatively measured by gamma spectroscopy. The number of Gd^{3+}-complexes per nanoparticle was determined from the ratio of the concentrations of Gd^{3+} and nanoparticles in the emulsion.

2.2. Relaxivity

Gd-DTPA-BOA, Gd-MeO-DOTA-PE and Gd-MeO-DOTA-triglycine-PE nanoparticle emulsions were diluted with distilled deionized water in ratios of 1:10, 1.5:10, 2:10, 2.5:10 and 3:10. The proton longitudinal and transverse relaxation rates ($1/T_1$ and $1/T_2$, respectively) of each sample were measured at 40 °C on an MQ20 Minispec NMR Analyzer (Bruker, Inc.) at a field strength of 0.47 T [11]. T_1 was measured with an inversion recovery sequence with 10 inversion delay values and T_2 was measured with a Carr–Purcell–Meiboom–Gill (CPMG) sequence [15,16]. The relaxivities (i.e., r_1 and r_2) were calculated from the slope of the linear least squares regression of relaxation rate vs. Gd^{3+}, i.e. ion relaxivity, or nanoparticle, i.e. particle relaxivity, concentrations and are reported in units of $(s \cdot mM)^{-1}$.

2.3. Transmetallation

Transmetallation of the gadolinium ion from the chelate was measured as described by Laurent et al., using zinc as the competing ionic species [14]. Transmetallation of a soluble, paramagnetic gadolinium complex with zinc ions in a phosphate-buffered solution releases Gd^{3+} and forms $GdPO_4$. $GdPO_4$ has very low solubility and no influence on the longitudinal relaxation rate. The proton relaxation rate decreases in proportion to the amount of Gd^{3+} released from the chelate. The temporal evolution of r_1 over time is related to the kinetics of the transmetallation reaction, whereas the steady-state value reflects the thermodynamic stability of the system.

Gd-DTPA-BOA, Gd-MeO-DOTA-PE and Gd-MeO-DOTA-triglycine-PE samples were diluted in PBS. The relaxation rate was measured at 0.47 T and 40 °C before and up to 72 h after addition of $ZnCl_2$. All samples were maintained at 40 °C in a dry block between measurements. As previously described [14], each sample had equivalent concentrations of Zn^{2+} and Gd^{3+}.

3. Results

All nanoparticle formulations were very similar with respect to their physical and chemical properties. The nominal diameters were very similar, ranging from 190 to 210 nm, with nearly identical size distributions. All formulations contained very similar concentrations of gadolinium, and therefore each formulation had a similar number of Gd^{3+}-complexes per particle (49,000–50,000).

The ionic r_1 relaxivity (Table 1) of the prototype Gd-DTPA-BOA nanoparticles was very high (21.3 $s \cdot mM^{-1}$) as reported in previous publications [5,11]. This relaxivity was further improved by substitution with either of the DOTA chelates (Gd-MeO-DOTA-PE: $r_1 = 29.8\,s \cdot mM^{-1}$; Gd-MeO-DOTA-triglycine-PE: $r_1 = 33.0\,s \cdot mM^{-1}$). In the present experiment particulate relaxivities were determined to be: Gd-DTPA-BOA, 1,260,000 $(s \cdot mM)^{-1}$; Gd-MeO-DOTA-PE, 1,470,000 $(s \cdot mM)^{-1}$; Gd-MeO-DOTA-triglycine-PE, 1,780,000 $(s \cdot mM)^{-1}$ (Table 1).

Using zinc as a competing species, longitudinal relaxivity of all three paramagnetic nanoparticle formulations decreased. The r_1 of Gd-DTPA-BOA nanoparticles decreased quickly and dramatically after the addition of $ZnCl_2$, suggesting rapid transmetallation as expected with the linear chemistry of the chelate and the compromise of two coordination bonds imparted by the lipid modification [13]. The gadolinium displacement from the DOTA-based nanoparticles by zinc was markedly less, which was consistent with improved stability of the Gd-MeO-DOTA complex. The retained gadolinium at equilibrium (Fig. 2) was much higher for the two Gd-MeO-DOTA ligands (91%) compared to the Gd-DTPA chelate (75%).

4. Discussion

We have utilized relaxivity and transmetallation measurements to evaluate two new paramagnetic nanoparticle formulations for MR molecular imaging. The Gd-MeO-DOTA-PE and Gd-MeO-DOTA-triglycine-PE nanoparticles were compared to our Gd-DTPA-BOA prototype formulation in terms of particle size, metal stability and relaxivity. In general, the increased relaxivity and decreased transmetallation characteristics of the new MeO-DOTA-PE-based nanoparticle formulations were favorable enhancements over the first-generation Gd-DTPA-BOA nanoparticles.

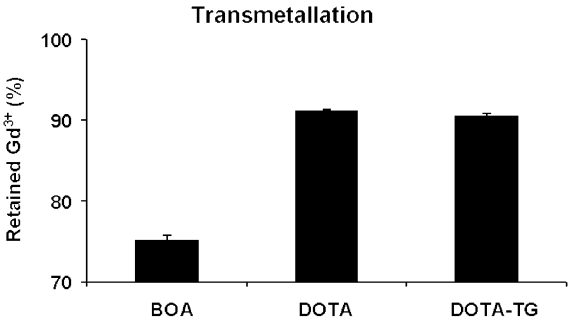

Fig. 2. Transmetallation of Gd-DTPA-BOA, Gd-MeO-DOTA-PE and Gd-MeO-DOTA-triglycine-PE nanoparticles at equilibrium after addition of $ZnCl_2$.

Table 1

Chelate	$[Gd^{3+}]$ (mM)	Particle diameter (nm)	Ionic relaxivity $(s \cdot mM\ Gd^{+3})^{-1}$		Particle relaxivity $(s \cdot mM\ particle)^{-1}$	
			r_1	r_2	r_1	r_2
Gd-DTPA-BOA	5.47	190	21.3	23.8	1,260,000	1,410,000
Gd-MeO-DOTA-PE	4.57	190	29.8	35.3	1,470,000	1,740,000
Gd-MeO-DOTA-triglycine-PE	3.70	210	33.0	38.6	1,780,000	2,080,000

Ion-based and particle-based relaxivities of three paramagnetic nanoparticle formulations r_1, longitudinal relaxivity; r_2, transverse relaxivity.

We have previously reported increased relaxivity when Gd-DTPA paramagnetic chelates utilized a PE anchor [11]. In that study, variable-field relaxometry measurement showed that Gd-DTPA-PE nanoparticles had faster water exchange relative to the original Gd-DTPA-BOA agent. This improved water interaction was proposed to result from the extended position of the metal chelate beyond the lipid surface. The improved relaxivity demonstrated in the present study was consistent with previous results and also likely reflects improved water exchange/accessibility afforded by displacement of the Gd-MeO-DOTA complex beyond the lipid surface. The enhanced relaxivity (~10%) measured in Gd-MeO-DOTA-triglycine-PE nanoparticles compared to Gd-MeO-DOTA-PE nanoparticles presumably resulted from slight further improvements in water exchange facilitated by the triglycine spacer. Although an optimal distance of chelate displacement from the lipid surface has not been determined, the surface separation created by the tripeptide spacer may approach a limit for increased relaxivity.

Previous investigators have shown that DTPA transmetallation decreases proportionately with the loss of metal coordinate bonds through the coupling of lipophilic linkers [13]. Although the diacyl lipophilic DTPA had the greatest transmetallation potential, the monosubstituted ligand also displayed significant metal displacement potential. Other investigators have developed DTPA chelates, which do not involve the coordinate bonds retaining gadolinium, e.g., benzyl-DTPA [17]. However, given the anticipated extended biological half-life of gadolinium in molecular imaging applications, we elected to utilize macrocyclic DOTA-based chelates, which are well known to retain gadolinium much more avidly than DTPA [14].

Methoxy DOTA lipid chelates utilized in this study preserved the coordination of gadolinium to the chelate while providing a reactive side group, i.e., isothiocyanate, for reaction with the terminal amines of phosphatidyl ethanolamine or the peptide derivative. Our data reveal the improved retention of metal DOTA nanoparticles in comparison with Gd-DTPA-BOA nanoparticles. In contradistinction to the earlier report of Laurent et al. [14], we measured greater decreases in relaxivity with the addition of zinc. These differences could relate to differences in interactions of Gd-DOTA vs. Gd-MeO-DOTA, masking of the metal by zinc, or unknown interactions between zinc, the Gd-MeO-DOTA chelate and the lipid surface of the particles.

We have recently developed theoretical and experimental methods to determine the minimum detection limit of targeted paramagnetic nanoparticles [12]. With the Gd-DTPA-BOA nanoparticles, we have shown diagnostic contrast-to-noise ratios (CNR > 5) at 1.5 T with concentrations around 100 pM. The increased relaxivity of the MeO-DOTA chelates in the current study should lower the detection limit by ~25%, allowing molecular imaging of sparser molecular targets or earlier stages of disease.

In conclusion, we have demonstrated that paramagnetic nanoparticles based on MeO-DOTA phosphatidylethanolamine chelates have improved relaxivity and diminished transmetallation in comparison with our initial Gd-DTPA-BOA-based agent. As we have previously noted, short extension of the paramagnetic chelate from the lipid nanoparticle surface through the use of a phospholipid anchor improved relaxivity, which was further enhanced by the addition of an intervening triglycine spacer. Transmetallation potential from the lipophilic paramagnetic chelates was greatly reduced through the use of MeO-DOTA-based chelates, which permitted coupling of the lipid anchor without compromise to the metal coordination chemistry of the ligand. In combination, the well-documented stability advantages of the DOTA chelates and their improved relaxivity afforded by extension of the chelate from the particle surface promise to improve the safety and efficacy of this novel molecular imaging agent.

Acknowledgements

We acknowledge grant support from the National Institutes of Health (HL-42950, HL-59865 and NO1-CO-07121), the American Heart

Association, the Barnes-Jewish Hospital Research Foundation and Philips Medical Systems.

References

[1] R. Weissleder, Radiologe 212 (1999) 609.
[2] H. Gupta, R. Weissleder, Magn. Reson. Imaging Clin. N. Am. 4 (1996) 171.
[3] R. Lauffer, T. Brady, Magn. Reson. Imaging 3 (1985) 11.
[4] D. Sipkins, D. Cheresh, M. Kazemi, et al., Nat. Med. 4 (1998) 623.
[5] S. Flacke, S. Fischer, M. Scott, et al., Circulation 104 (2001) 1280.
[6] P. Winter, S. Caruthers, A. Kassner, et al., Cancer Res. 63 (2003) 5838.
[7] P. Winter, A. Morawski, S. Caruthers, et al., Circulation 108 (2003) 2270.
[8] L. Bryant, M. Brechbiel, C. Wu, et al., J. Magn. Reson. Imaging 9 (1999) 348.
[9] Y. Manabe, C. Longley, P. Furmanski, Biochim. Biophys. Acta. 883 (1986) 460.
[10] G. Lanza, C. Lorenz, S. Fischer, et al., Acad. Radiol. 5 (Suppl 1) (1998) s173.
[11] P. Winter, S. Caruthers, X. Yu, et al., Magn. Reson. Med. 50 (2003) 411.
[12] A. Morawski, P. Winter, K. Crowder, et al., Magn. Reson. Med. 51 (2004) 480.
[13] A. Sherry, W. Cacheris, K. Kuan, Magn. Reson. Med. 8 (1988) 180.
[14] S. Laurent, L.V. Elst, F. Copoix, et al., Invest. Radiol. 36 (2001) 115.
[15] H. Carr, E. Purcell, Physiol. Rev. 94 (1954) 630.
[16] S. Meiboom, D. Gill, Rev. Sci. Instrum. 29 (1958) 688.
[17] R. Sharkey, C. Motta-Hennessy, O. Gansow, et al., Int. J. Cancer 46 (1990) 79.